EXPERT OPINION

Multifunctional nanoparticles of Fe_3O_4@SiO_2(FITC)/PAH conjugated the recombinant plasmid of pIRSE2-EGFP/$VEGF_{165}$ with dual functions for gene delivery and cellular imaging

Yiyao Liu†, Mengran Shi, Mingming Xu, Hong Yang & Chunhui Wu
†*University of Electronic Science and Technology of China, School of Life Science and Technology, Department of Biophysics, Chengdu, Sichuan, P.R. China*

Objectives: Technologies to increase tissue vascularity are critically important to the fields of tissue engineering and cardiovascular medicine. Angiogenic factors, like VEGF, have been widely investigated to induce vascular endothelial cell proliferation and angiogenesis for establishing a vascular network. However, effective transport of VEGF gene to target cells with minimal side effects remains a challenge despite the use of unique viral and non-viral delivery approaches.

Methods: This study presents a novel gene delivery system of fluorescein isothiocyanate (FITC) doped and poly(allylamine hydrochloride) (PAH) grafted Fe_3O_4@SiO_2 nanoparticles, which allows efficient loading of pVEGF to form Fe_3O_4@SiO_2(FITC)/PAH/pVEGF nanocomplexes for VEGF gene delivery and cellular imaging.

Results: The nanocomplexes maintain their superparamagnetic property in the silica composites at room temperature, reaching a saturation magnetization value of 5.19 emu/g of material, and no appreciable change in magnetism even after PAH modification. The quantitative analysis of cellular internalization into the living human umbilical vein endothelial cells (HUVECs) demonstrated that the Fe_3O_4@SiO_2(FITC)/PAH/pVEGF nanocomplexes could be entirely internalized by HUVECs, and exhibit high VEGF gene expression and an innocuous toxic profile. The magnetic resonance (MR) images showed that the superparamagnetic iron oxide core of Fe_3O_4@SiO_2(FITC)/PAH/pVEGF nanocomplexes could also act as a contrast agent for MR imaging. This property provides a benefit for monitoring gene delivery.

Conclusion: These data highlight multifunctional Fe_3O_4@SiO_2(FITC)/PAH/pVEGF nanocomplexes as an attractive platform for gene delivery of angiogenesis, and also making it a potential candidate of nanoprobes for cellular fluorescent imaging or MR imaging.

Keywords: cell imaging, core-shell nanoparticles, gene delivery, PAH, VEGF

Expert Opin. Drug Deliv. (2012) 9(10):1197-1207

1. Introduction

Technologies to enhance angiogenesis and arteriogenesis are greatly needed in cardiovascular medicine and tissue engineering [1,2]. Limited options currently exist to increase tissue vascularity in a controlled manner. Gene therapy offers a potential method to cure inherited or acquired diseases by transferring exogenous nucleic

informa
healthcare

10.1517/17425247.2012.709845 © 2012 Informa UK, Ltd. ISSN 1742-5247

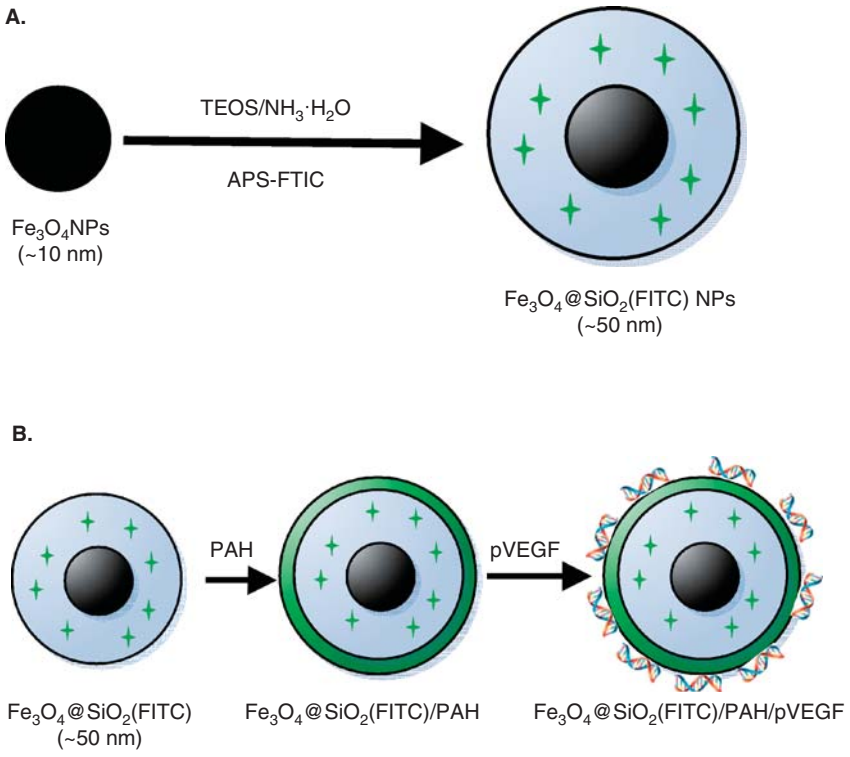

Figure 1. Preparation of Fe_3O_4@SiO_2(FITC)/PAH/pVEGF nanocomplexes. A. Schematic diagram of Fe_3O_4@SiO_2(FITC) nanoparticles synthesized by reverse microemulsion. **B.** Surface modification with PAH for electrostatic absorption of the recombinant plasmid of pIRSE2-EGFP/$VEGF_{165}$ (pVEGF) to form Fe_3O_4@SiO_2(FITC)/PAH/pVEGF nanocomplexes.

acids into cells to alter protein expression profiles. Although recombinant viruses are currently used for this purpose because of their high transfection activity, the use for non-viral vectors is still desired from the viewpoint of safety [3]. The application of non-viral systems for gene delivery is being increasingly advocated because of their low immunogenicity, unlimited payload capacity, absence of endogenous virus recombination, low production cost and reproducibility [4]. Several promising nanoparticle delivery systems have been proposed for gene therapy [5-7]. For example, superparamagnetic iron oxide nanoparticles (SPIO) have been recognized as a promising tool for the site-specific delivery of drugs/genes and diagnostics agents [8-10].

Vasculogenic agent of VEGF has been previously shown to enhance revascularization *in vivo*. The sustained expression of VEGF may be necessary for the maintenance of stable neovessels. The use of human VEGF as a potential stimulant in therapeutic angiogenesis has been widely demonstrated. Many nanocarriers have been investigated and applied in VEGF gene delivery [11], among them, SPIO is an attractive delivery vehicle because of its excellent biocompatibility, high safety profile and widespread use in medicine. Most of the earlier works reported so far regarding magnetic nanoparticle-mediated gene delivery, demonstrated mere mixing of the magnetic nanoparticles with cationic polymers such as polyethylenimine (PEI), diethylaminoethyl-dextran (DEAE-dextran) in order to coat the magnetic nanoparticles to enrich their functions [8,9,12,13]. Following this concept, combining different materials will enable the development of multifunctional nanomedical platforms for multimodal imaging or simultaneous diagnosis and therapy [14-18]. Recent advances in nanoscience and biomedicine have expanded the ability to design and construct multifunctional nanoparticles that combine targeting, therapeutic and diagnostic functions within a single nanoscale complex. The theranostic capabilities of multifunctional nanoparticles have attracted tremendous attention over the past decade, and have emerged as a promising tool for some disease therapy and bioimaging enhancement [19-21]. Sumer and Gao coined the term 'theranostic nanomedicine' to denote such kind of integration of diagnostic imaging capability with therapeutic interventions [22]. In order to realize this goal, one of the key issues is to reasonably design and fabricate the multifunctional nanoparticles. In the synthetic strategy, silica was selected for surface coating of SPIO nanoparticles because dye molecules can be easily incorporated into a silica shell, and silica is quite biocompatible and resistant to biodegradation in the biological environments [14,23,24]. Although silica can be easily surface functionalized, it is still difficult for conjugating genes due to the negative charges of silica surfaces. Poly(allylamine hydrochloride) (PAH) is a polyelectrolyte material that has high good water solubility and high-density amine-rich polycations

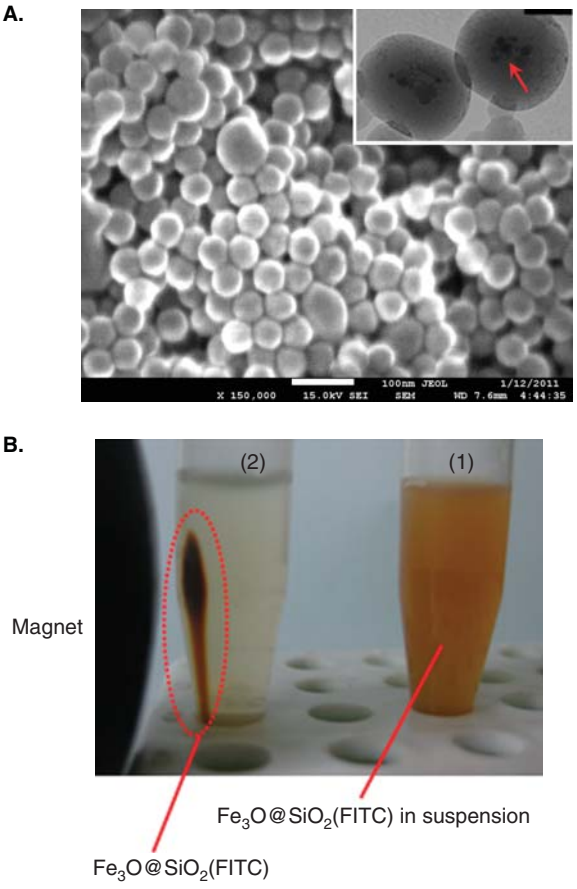

Figure 2. A. Scanning electron micrograph of Fe_3O_4@SiO_2(FITC)/PAH nanoparticles. Insert: higher-magnification image of transmission electron microscope. Scale bar = 100 nm. **B.** Photographs of aqueous suspension of Fe_3O_4@SiO_2(FITC)/PAH nanoparticles before (1) and after (2) magnetic capture.

at physiological pH values. Polyelectrolyte multilayers are efficient in the release of naked DNA and the subsequent *in vitro* transfection [25]. Hence, in this study the authors will combine the merits of the two materials to engineer a new type of multifunctional nanoparticles.

The goals of the present studies were to develop a formulation approach to engineer a novel type of multifunctional nanoparticle as theranostic agent for non-viral gene transfer and cellular imaging. The authors further characterized with respect to their morphology, fluorescent and magnetic properties, and also studied the VEGF gene delivery characteristics including cellular internalization and VEGF expression in cultured endothelial cells. In addition, they demonstrated that the fabricated multifunctional nanoparticles of Fe_3O_4@SiO_2(FITC)/PAH/pVEGF nanocomplexes have fluorescent and magnetic properties, and could be used as both fluorescent and magnetic imaging probes in cellular level. It is expected to be an important candidate theranostic system for biomedical applications.

2. Materials and methods

2.1 Materials

PAH with an average molecular weight of ~56,000, polyoxyethylene(5) nonylphenylether (Igepal CO-520), tetraethyl orthosilicate (TEOS), 3-aminopropyltrimethoxysilane (APS), fluorescein isothiocyanate (FITC) and sodium silicate solution ($Na_2O(SiO_2)_{3-5}$, 27 wt% SiO_2) were obtained from Sigma-Aldrich (St. Louis, MO, USA). Iron oxide nanoparticles (10 nm) were purchased from Nanjing Emperor Nano Material Co., Ltd. (Nanjing, China). Cell culture medium RPMI 1640, newborn calf serum (NCS) and trypsin were purchased from Gibco (Grand Island, NY, USA). The recombinant plasmid of pIRSE2-EGFP/$VEGF_{165}$ (pVEGF) was obtained from Fungenome Co., Ltd. (Beijing, China). All the other chemicals used were of analytical reagent grade and used without further purification unless identified.

2.2. Preparation of Fe_3O_4@SiO_2(FITC)/PAH/pVEGF nanocomplexes

FITC (5 mg) was conjugated with APS (10 µl) in anhydrous ethanol (3 ml) by an addition reaction of isothiocyanate group with amine group. The reaction was carried out in dark for 12 h by slight stirring. The reaction solution of FITC–APS conjugates was then stored at 4°C [23].

Fe_3O_4@SiO_2(FITC)/PAH/pVEGF nanocomplexes were prepared by an improved microemulsion method [25-27]. Briefly, Fe_3O_4 powder (0.5 mg) was dissolved in cyclohexane (7.7 ml) at room temperature. Then, Triton X-100 (2 g), hexanol (1.6 ml) and H_2O (0.34 ml) were added with stirring to generate the microemulsion system. Then, TEOS (40 µl) was added to the mixture. Six hours later, 100 µl aqueous ammonia (28 ~ 30 wt%) was introduced to initiate the TEOS hydrolysis. After 24 h, 30 µl TEOS and 20 µl *N*-1-(3-trimethoxysilylpropyl)-*N*′-fluoresceyl thiourea (FITC-APS) ethanolic solution were added under stirring for 24 h. Finally, ethanol was added to destabilize the microemulsion system. The FITC-incorporated and silica-coated core-shell Fe_3O_4@SiO_2(FITC) nanoparticles were isolated via centrifugation and washed in sequence with ethanol and Milli-Q water to remove any surfactant and unreacted reactants.

PAH (6 mg) was dissolved in 1 ml of Milli-Q water. The PAH solution was mixed with the Fe_3O_4@SiO_2(FITC) nanoparticle suspension (1 ml), and rotated for 2 h at a speed of 180 rpm to allow PAH to graft onto the surface of Fe_3O_4@SiO_2(FITC) nanoparticles. Unbound PAH was removed by dialyzing the mixture against 2 l of water with several water replacements for 24 h using a dialysis membrane with a 100,000 Dalton cut-off (MYM Technologies Ltd., Hyderabad, Andhra Pradesh, India). The suspension containing Fe_3O_4@SiO_2(FITC)/PAH nanoparticles were lyophilized and vacuum-dried at -4°C.

Fe_3O_4@SiO_2(FITC)/PAH nanoparticles were then dissolved in distilled water at a final concentration of 1 mg/ml. The recombinant plasmid of pVEGF was incubated in the Fe_3O_4@SiO_2(FITC)/PAH suspension for 30 min at room

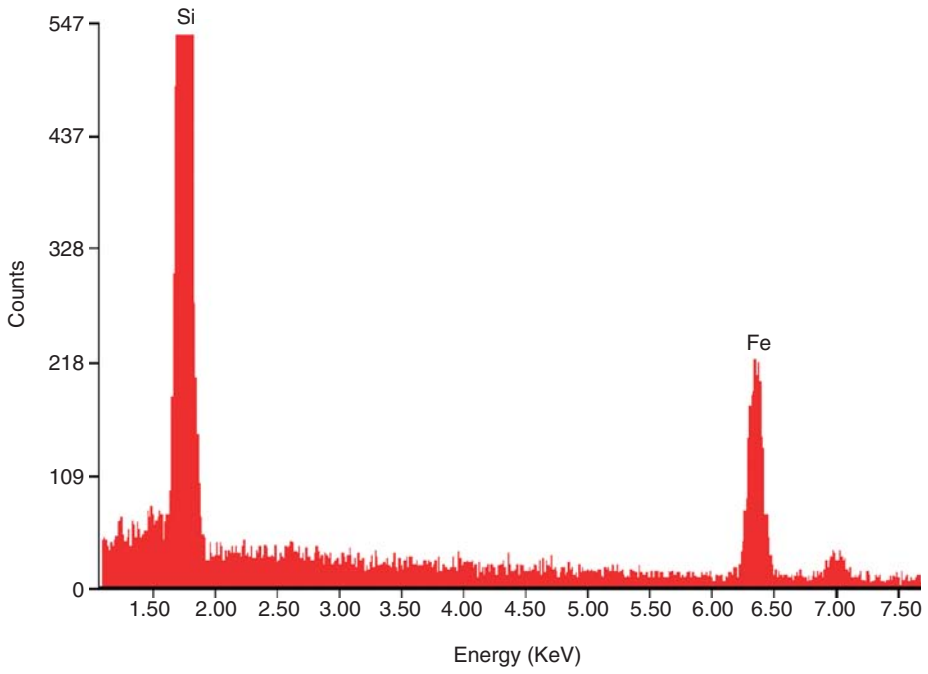

Figure 3. EDX of Fe_3O_4@SiO_2(FITC) showing the presence of Fe_3O_4.

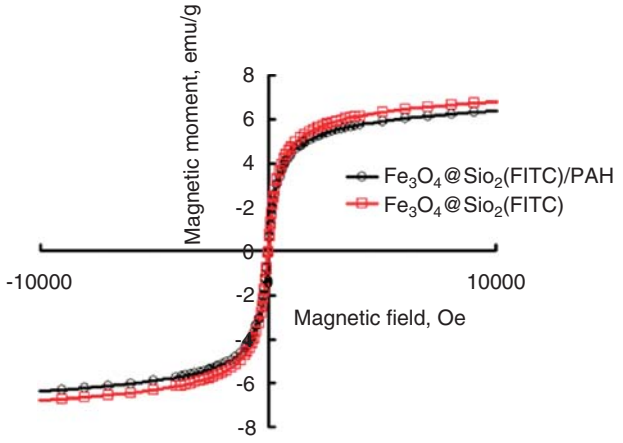

Figure 4. Field-dependent magnetization curves of Fe_3O_4@-SiO_2(FITC) and Fe_3O_4@SiO_2(FITC)/PAH at room temperature.

temperature to form Fe_3O_4@SiO_2(FITC)/PAH/pVEGF complexes by electrostatic absorption at various weight ratios (Fe_3O_4@SiO_2(FITC)/PAH:pVEGF) of 100:1, 50:1 and 20:1. The synthetic procedure for the Fe_3O_4@SiO_2(FITC)/PAH/pVEGF complexes is shown in **Figure 1**.

2.3 Characterization

Scanning electron microscopy (SEM) measurements were performed on a JSM-6490LV (JEOL, Tokyo, Japan) microscope. Transmission electron microscopy (TEM) experiments were performed on JEM-100CX (JEOL, Tokyo, Japan) electron microscopes with an acceleration voltage of 200 kV. Samples were prepared by drying a drop of the dilute solutions onto 300-mesh carbon-coated copper grids which were allowed to dry completely at room temperature. The presence of Fe_3O_4 was evidenced by energy-dispersive X-ray (XRD) analysis.

2.4 Magnetization curves

Magnetic measurements of samples were performed on a superconducting quantum interference device (SQUID) magnetometer (MPMS5S, Quantum Design). For measurement, about 10 mg of powder samples was inserted in a gelatin capsule at room temperature. The magnetic hysteresis loop was measured at room temperature.

2.5 Cell culture

Endothelial cells of human umbilical vein endothelial cell (HUVEC)-CS were routinely cultured in RPMI1640 supplemented with 10% NCS, 100 U/ml penicillin and 100 mg/ml streptomycin. For another endothelial cells of EA.hy926, the cells were cultured in RPMI 1640 containing 10% newborn calf serum, 100 U/ml penicillin and 100 mg/ml streptomycin, 2% $NaHCO_3$, 20 mM 2-[4-(2-hydroxyethyl)-1-piperazine] ethanesulfonic acid and 2% HAT (hypoxanthine, aminopterin and thymidine) supplement. All the cells were incubated at 37°C in a humidified CO_2 atmosphere. The medium was changed every third day.

2.6 Flow cytometry and cellular uptake assay

To observe cellular uptake of nanoparticles, EA.hy926 cells were seeded in 12-well plates for 24 h at an initial cell density

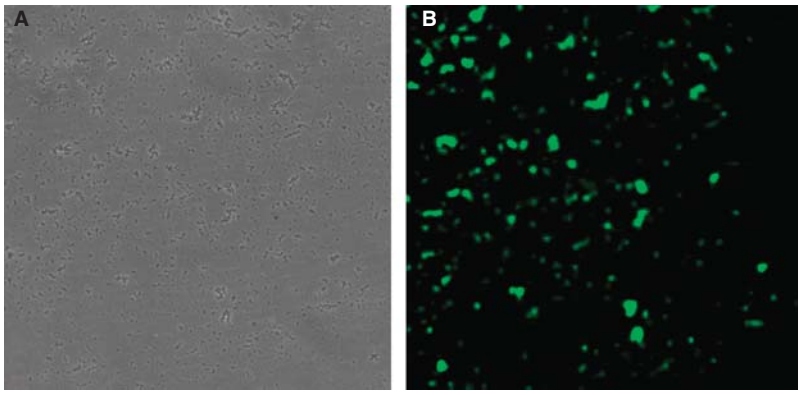

Figure 5. Light (**A**) and fluorescence (**B**) micrographs of aqueous suspension of Fe_3O_4@SiO_2(FITC) nanoparticles in solution.

of 1×10^5 cells/well. Fe_3O_4@SiO_2(FITC)/PAH nanoparticles were prepared at varying weight ratios of Fe_3O_4@SiO_2(FITC) to PAH (30:1, 20:1 and 15:1). The final concentrations of Fe_3O_4@SiO_2(FITC)/PAH nanoparticles were 100 μg/ml. At the time of cellular uptake experiment, the medium in each well was replaced with fresh serum-free medium. The Fe_3O_4@SiO_2(FITC)/PAH nanoparticles were incubated with cells at 37°C for 6 h. The medium containing Fe_3O_4@SiO_2(FITC)/PAH nanoparticles was removed by aspiration and the cells were washed with phosphate-buffered saline (PBS) for three to five times, harvested by trypsin enzyme and neutralized with serum-containing medium. After centrifugation at 200 *g* for 5 min, cells were resuspended in 500 μl PBS. Samples were kept in ice and analyzed by the flow cytometer (FACSCanto II; BD Biosciences, Franklin Lakes, NJ, USA) at a minimum of 1×10^4 cells. The uptake efficiency was calculated as the ratio of the number of fluorescence-labeled cells (fluorescent nanoparticles-endocytosed cells) to the initial cultured cells. To investigate the impact of Fe_3O_4@SiO_2(FITC)/PAH nanoparticles concentration on cellular uptake, the authors used the Fe_3O_4@SiO_2(FITC) nanoparticles at the weight ratio of 20:1 to incubate with EA.hy926 cells at the final concentration of 100, 67 and 33 μg/ml. The next experiment is the same manner as described above. All the assays were performed in duplicate.

2.7 Cell proliferation assay

For the *in vitro* time-course cell proliferation assay experiments, EA.hy926 cells were seeded in 96-well plates at an initial density of 2×10^4 cells/well. At the same time, EA.hy926 cells were seeded in 24-well plates at a density of 5×10^4 cells/well and then transfected with Fe_3O_4@SiO_2(FITC)/PAH/pVEGF nanocomplexes. The weight ratios of Fe_3O_4@SiO_2(FITC)/PAH to pVEGF were 100:1, 50:1 and 20:1. The final concentration of pDNA was 1 μg/ml in the each well. Cells transfected with Lipofectamine2000 (Lip) (final concentration 0.5μl/ml) were used as the positive control, and untreated cells (equal culture medium addition) were used as a negative control for calibration and normalization. EA.hy926 cells were incubated with Fe_3O_4@SiO_2(FITC)/PAH/pVEGF nanocomplexes for 48 h, and then 300 μl culture medium from transfected cells was collected and transferred to the new cultured EA.hy926 cells in 96-well plates. Cell proliferation was measured by WST-8 assay at the culture time of 24, 48 and 72 h. All the assays were performed in triplicate.

2.8 VEGF expression assay

The VEGF therapeutic protein secreted from endothelial cells was measured using a Quantikine Human VEGF immunoassay ELISA kit [28]. EA.hy926 cells were seeded in 24-well plates at an initial cell density of 5×10^4 cells/well. After 24 h, cells were transfected by Fe_3O_4@SiO_2(FITC)/PAH/pVEGF nanocomplexes at a wt/wt (Fe_3O_4@SiO_2(FITC)/PAH to pVEGF) ratio of 100:1 and 50:1. Non-transfected and Lip-transfected cells were used as control. Six hours after transfection, the cultured serum-free medium was replaced with 500 μl fresh medium containing serum. The culture medium was collected 30 and 60 h in post-transfection and kept at -20°C until use. ELISA assay was performed according to the instructions from manufacturer's protocol. All the assays were performed in triplicate.

2.9 Fluorescent tracking and imaging

Endothelial cells of EA.hy926 were incubated with Fe_3O_4@SiO_2(FITC)/PAH/pVEGF nanocomplexes for 6 h in 24-well plates. The cells were washed with PBS repeatedly until no fluorescence was detectable in the supernatant, and then fresh medium was added. Finally, the cells were observed under a fluorescent microscope (Nikon TE2000-U, Tokyo, Japan) with various magnifications. The cellular distribution of Fe_3O_4@SiO_2(FITC)/PAH/pVEGF nanocomplexes could be detected through FITC fluorescence after particles internalization.

2.10 Relaxation measurement and MR imaging

Endothelial cells of EA.hy926 and HUVEC-CS were incubated with Fe_3O_4@SiO_2(FITC)/PAH/pVEGF nanocomplexes with various final concentrations of 0, 10, 50, 100 and 160 μg/ml for a given time at 37°C in cell culture medium. The cells

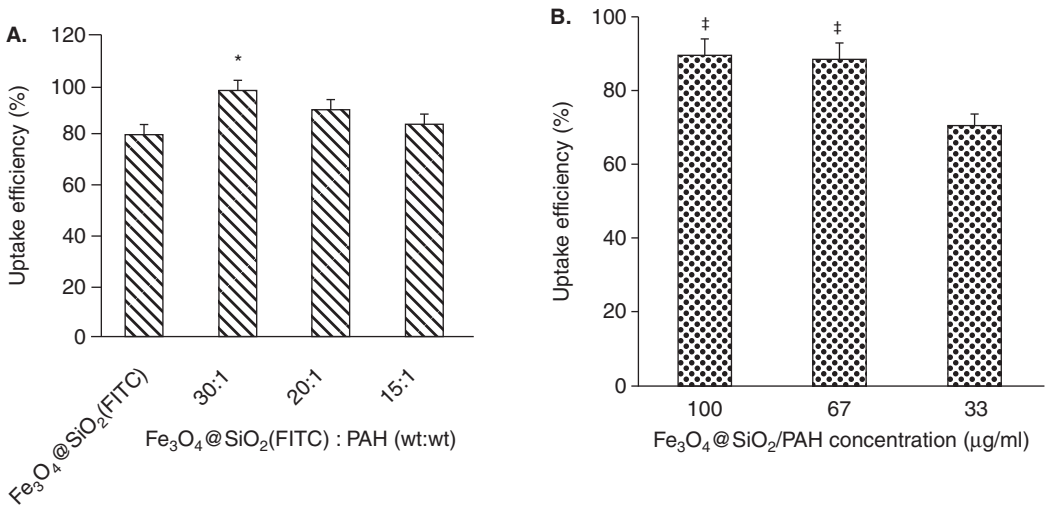

Figure 6. A. Quantitative cellular delivery (uptake) assessment of Fe_3O_4@SiO_2(FITC)/PAH nanoparticles with various weight ratios of Fe_3O_4@SiO_2(FITC):PAH into endothelial cells (EA.hy926) detected by flow cytometry. **B.** Cellular uptake efficiency by endothelial cells treated with different concentrations of Fe_3O_4@SiO_2(FITC)/PAH nanoparticles (weight ratio of Fe_3O_4@SiO_2(FITC):PAH is 20:1). The uptake efficiency was calculated as the ratio the number of fluorescence labeled cells (fluorescent nanoparticles-endocytosed cells) to the initial cultured cells.

*$p < 0.05$ for ratio 30:1 vs. Fe_3O_4@SiO_2(FITC).

‡$p < 0.05$ for the concentrations of 67 and 100 μg/ml vs. the concentration of 33 μg/ml of Fe_3O_4@SiO_2(FITC)/PAH nanoparticles.

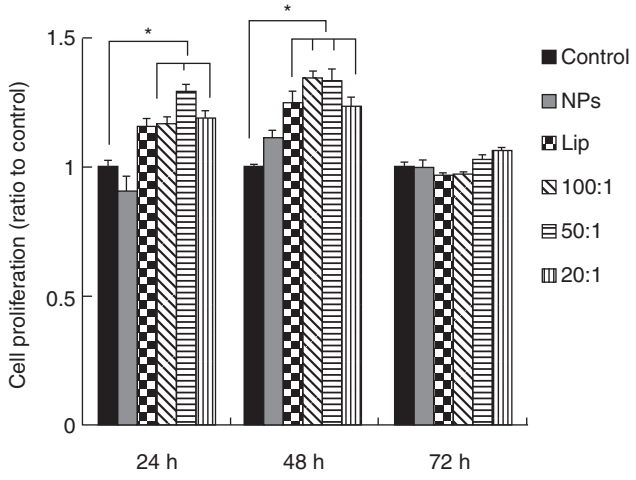

Figure 7. Proliferation of endothelial cells treated with Fe_3O_4@SiO_2(FITC)/PAH/pVEGF nanocomplexes with different weight ratios of Fe_3O_4@SiO_2(FITC)/PAH nanoparticles: pVEGF, in comparison with the control (equal culture medium addition), NPs (Fe_3O_4@SiO_2(FITC)/PAH nanoparticles addition) and the commercial available transfection agent of Lipofectamine2000 (Lip).

*$p < 0.05$ indicates significant difference vs. control.

were then washed three times with PBS solution, collected and suspended in 1.5 ml of PBS buffer containing 1% agarose. MR imaging experiments were performed in a 7.0-T Bruker magnet (Bruker Medical Systems, Karlsruhe, Germany). The T_2-weighted images were acquired using spin-echo imaging sequence. The relaxivities (R_2) were obtained from the linear regressions. R_2 is defined as $1/T_2$ with unit of s^{-1}.

2.11 Presentation of data and statistical analysis

Data were presented as mean ± standard deviation (SD). The statistical significance of differences was tested using one-way ANOVA followed by Bonferroni tests and $p < 0.05$ was considered significant.

3. Results and discussion

The preparation of Fe_3O_4@SiO_2(FITC) nanoparticles, using an improved microemulsion method, immediately followed by coating with the polyelectrolyte material of PAH, resulted in easily dispersed, non-agglomerated Fe_3O_4@SiO_2(FITC)/PAH nanoparticles. SEM and dynamic light scattering analyses of these nanoparticles revealed that they were spherical and uniform with 50 ± 3 nm in diameter (**Figure 2A**). TEM indicated that the magnetic nanocrystal embedded in silica still retained its original crystallinity after silica coating and surfactant extraction. One or more magnetic nanocrystals were embedded in a Fe_3O_4@SiO_2(FITC)/PAH nanoparticle. In PBS solution at room temperature, the Fe_3O_4@SiO_2(FITC)/PAH nanoparticles remained well dispersed without a magnetic field in the PBS of the polymerase chain reaction tube (**Figure 2B**(1)). However, the Fe_3O_4@SiO_2(FITC)/PAH nanoparticles collected at the side wall soon after the magnet was placed (**Figure 2B**(2)), which also demonstrated that the core-shell nanoparticles were successfully synthesized, and

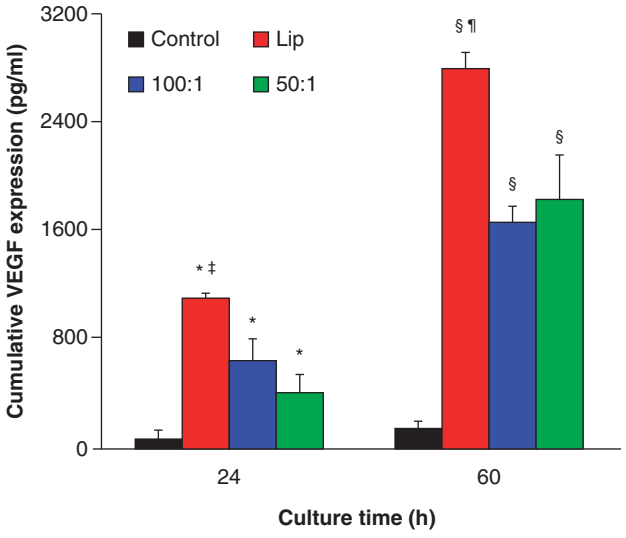

Figure 8. The cumulative amount of VEGF expressed and released from the transfected endothelial cells of EA.hy926 with two Fe_3O_4@SiO_2(FITC)/PAH:pVEGF ratios of 50:1 and 100:1 over a time period of 60 h, in comparison with the control (equal culture medium addition) and the commercial transfection agent of Lipofectamine2000 (Lip). ELISA was performed using the Quantikine human VEGF ELISA kit, as shown in Section 2.

*$p < 0.05$, compared with control at 24 h.

‡$p < 0.01$, compared with control at 60 h.

§$p < 0.01$, compared with control at 60 h.

¶$p < 0.05$, compared with Fe_3O_4@SiO_2(FITC)/PAH/pVEGF (ratios 100:1 or 50:1) at 60 h.

the resultant nanocomposites can be manipulated by an external magnetic field. In order to further confirm whether the Fe_3O_4 nanocrystal was coated by a layer of silica shell, EDX method was also used as shown in **Figure 3**. The presence of silica and iron in the nanocomposite proves that core-shell Fe_3O_4@SiO_2 structure is formed. The thickness of the silica shell can be controlled by the microemulsion system. Shell thickness decreases with decreasing concentration of ammonium hydroxide and TEOS [29]. Thicker silica shell magnetite nanoparticles (up to 150 nm) can also be synthesized by adjusting the reaction agents (data not shown). In this study, 50 nm diameter is a suitable and desirable size for gene delivery because smaller particle size would be more easily and efficient at transfecting cells.

Magnetic properties of the magnetite silica composite were characterized by SQUID magnetometry. Both Fe_3O_4@SiO_2(FITC) and Fe_3O_4@SiO_2(FITC)/PAH nanoparticles exhibited superparamagnetic behavior at room temperature showing no significant hysteresis and a remnant magnetization (**Figure 4**). Compared with the bare Fe_3O_4 nanoparticles, the magnetization saturation value of Fe_3O_4@SiO_2(FITC) decreased from 51.8 (data not shown) to 6.8 emu/g due to the low density of the magnetic component in the core-shell nanostructure [30-32]. Of importance, there are no significant decrease for magnetization saturation values after PAH electrostatic absorption on the surface of Fe_3O_4@SiO_2(FITC) nanoparticles. For Fe_3O_4@SiO_2(FITC)/PAH nanoparticles, the magnetic moment first increased linearly, and then reached a magnetization saturation value of 6.36 emu/g. The specific magnetic susceptibility of the Fe_3O_4@SiO_2(FITC)/PAH nanoparticles was found to be better than that of other reports [9,29]. The superparamagnetic property at room temperature of Fe_3O_4@SiO_2(FITC)/PAH nanoparticles is an important parameter for biomedical applications.

To investigate whether the FITC molecules were embedded into the silica shells, the authors detected the fluorescence property of Fe_3O_4@SiO_2(FITC)/PAH nanoparticles in PBS solution. The fluorescence photograph of Fe_3O_4@SiO_2(FITC)/PAH nanoparticles in PBS solution is shown in **Figure 5B**. The encapsulation of FITC dye in Fe_3O_4@SiO_2/PAH nanoparticles endowed the nanoprobes with excellent fluorescent property. The authors observed that the Fe_3O_4@SiO_2(FITC)/PAH nanoparticles emitted strong green fluorescence in aqueous suspension. This observation further proves that the core-shell Fe_3O_4@SiO_2 and FITC are combined together. Other studies documented that silica shell or other materials shell did not alter the spectra characteristics of FITC dye [23,33].

To better explore the efficacy of cellular uptake, three weight ratios of 15:1, 20:1 and 30:1 of Fe_3O_4@SiO_2(FITC):PAH were prepared, and their abilities to be delivered into endothelial cells of EA.hy926 were compared. There were more than 85% uptake efficiencies regardless of the Fe_3O_4@SiO_2(FITC):PAH ratio (**Figure 6A**). For the weight ratio of 30:1, the uptake efficiencies reached about 98%. The authors also investigated the uptake efficiency of Fe_3O_4@SiO_2(FITC)/PAH nanoparticles (weight ratio 30:1) under various concentrations. It was found that the uptake efficiency was near 90% at the concentrations of 67 and 100 µg/ml. The previous data also showed that Fe_3O_4@-SiO_2(FITC)/PAH nanoparticles were very low cytotoxicity [25]. These data demonstrated that Fe_3O_4@SiO_2(FITC)/PAH was excellent delivery system. It has been reported that cells can internalize materials by several endocytotic processes such as clathrin-mediated endocytosis, caveolae-mediated endocytosis, macropinocytosis and so forth [34,35]. In their previous work, the authors demonstrated that the uptake of silica nanoparticles modified by PEG and folate was predominated by clathrin-mediated endocytosis and required the consumption of adenosine triphosphate (ATP) [36]. It is speculated that the uptake mechanism of Fe_3O_4@SiO_2(FITC)/PAH uptake may be similar.

In the previous studies, it was demonstrated that Fe_3O_4@SiO_2(FITC)/PAH nanoparticles could electrostatic absorb and protect the plasmid DNA containing the gene encoding the enhanced green fluorescent reporter protein (EGFP) [25]. Herein, the authors questioned whether Fe_3O_4@SiO_2(FITC)/PAH/pVEGF nanocomplexes can be effectively delivered into cells and promote cell proliferation. Therefore, endothelial cells of EA.hy926 were treated with Fe_3O_4@SiO_2(FITC)/PAH/

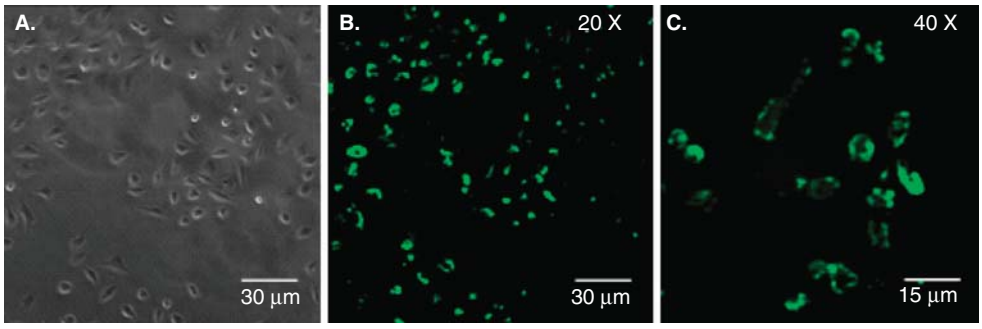

Figure 9. Fluorescent imaging and tracking of Fe_3O_4@SiO_2(FITC)/PAH/pVEGF nanoparticles in vascular endothelial cells in the presence of serum cultured for 6 h. (A) Light micrograph of Fe_3O_4@SiO_2(FITC) nanoparticles co-cultured with endothelial cells (EA.hy926) in culture medium. The internalization and intracellular tracking of Fe_3O_4@SiO_2(FITC)/PAH/pVEGF nanoparticles was assessed by an inverted fluorescence microscope under different magnifications of 20× **(B)** and 40× **(C)**.

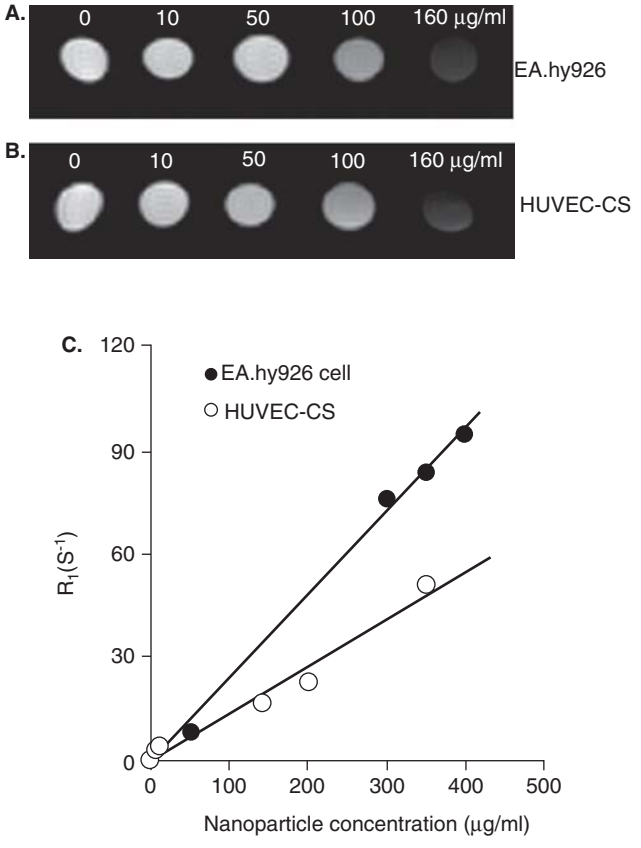

Figure 10. T_2-weighted images of EA.hy926 (A) and HUVEC-CS **(B)** incubated with Fe_3O_4@SiO_2(FITC)/PAH/pVEGF nanocomplexes showing the degree of uptake by cells and enhanced contrast provided by cellular uptake. **(C)** Relaxation (R_2) plot of Fe_3O_4@SiO_2(FITC)/PAH/pVEGF samples as a function of nanoparticle concentrations showing Fe_3O_4@SiO_2(FITC)/PAH/pVEGF retained good magnetism.

pVEGF nanocomplexes of different weight ratios of Fe_3O_4@SiO_2(FITC)/PAH nanoparticles:pVEGF at the same concentration. Fe_3O_4@SiO_2(FITC)/PAH/pVEGF nanocomplexes could obviously promote cell proliferation within 48 h, but there seems no significant difference at 72 h transfection (**Figure** 7). This phenomenon also exists for the commercial available transfection agent of Lip. It is reasonable to be understood that the above-mentioned transfection is transient transfection. The authors also found that there was no significant difference between nanocomplexes and Lip for cell proliferation. They then evaluated the cumulative amount of VEGF expressed and released from the transfected endothelial cells of EA.hy926. It was found that transfection by Fe_3O_4@SiO_2(FITC)/PAH/pVEGF nanocomplexes remarkably enhanced VEGF expression (**Figure 8**). For the Fe_3O_4@SiO_2(FITC)/PAH NPs:pVEGF ratio of 100:1, the cumulative VEGF expression in EA.hy926 cells was striking, and a 8.2- and 11-fold increase than that of the control after 24 and 60 h transfection, respectively. This result was attributed to the efficient delivery of Fe_3O_4@SiO_2(FITC)/PAH/pVEGF nanocomplexes into EA.hy926 cells. VEGF is a potent mitogen for endothelial cells *in vitro* and a key factor of angiogenesis *in vivo*. There is mounting evidence that VEGF may be a major regulator for cell proliferation. The authors' data demonstrated that Fe_3O_4@SiO_2(FITC)/PAH/pVEGF nanocomplexes exhibit excellent property in VEGF gene therapy *in vitro*.

Due to the fluorescent dye molecules of FITC doped into the silica shells, the authors could also detect the biodistribution of Fe_3O_4@SiO_2(FITC)/PAH/pVEGF nanocomplexes in the cells through fluorescence imaging. The cellular biodistribution of Fe_3O_4@SiO_2(FITC)/PAH/pVEGF nanocomplexes was verified by fluorescence microscopy following the incubation of cells with the nanoparticles in serum containing cell culture media for 24 h. Green fluorescence of FITC-doped Fe_3O_4@SiO_2(FITC)/PAH/pVEGF complexes was clearly observed in

cytoplasm (**Figure 9**). These data implied that Fe_3O_4@SiO_2 (FITC)/PAH/pVEGF nanocomplexes could be used as a fluorescent tracer for detection. To demonstrate *in vitro* multimodal cellular imaging, T_2-weighted MR imaging of Fe_3O_4@SiO_2 (FITC)/PAH/pVEGF nanocomplexes-labeled cell phantom were acquired (**Figure 10A**). As the concentration of the nanocomplexes was increased during the incubation, the T_2-weighted MR image was darkened for the two endothelial cell lines of EA.hy926 and HUVEC-CS. This demonstrates that the nanocomplexes can also be used as a probe for simultaneous T_2 MR imaging and optical fluorescence imaging. The authors further examined the relaxation (R_2) changes of Fe_3O_4@SiO_2(FITC)/PAH/pVEGF nanocomplexes after cellular uptake by endothelial cells of EA.hy926 and HUVEC-CS. It was found that the relaxivities (slopes of the R_2 vs. nanoparticle concentration curves) for the two endothelial cell lines of EA.hy926 and HUVEC-CS were a little different. It was speculated that it may be due to the cellular uptake difference of Fe_3O_4@SiO_2(FITC)/PAH/pVEGF nanocomplexes for the cells of EA.hy926 and HUVEC-CS. The authors' data demonstrated that Fe_3O_4@SiO_2(FITC)/PAH/pVEGF complexes can serve as good molecular imaging probe for both optical and magnetic contrast. In other words, dual-modality detections could be simultaneously achieved using a single nanomaterial.

4. Conclusions

In summary, the authors have developed a strategy for the synthesis of a multifunctional nanoparticle system of Fe_3O_4@SiO_2(FITC)/PAH/pVEGF, which simultaneously possesses dual functions for gene delivery and cellular imaging. The multifunctional nanoparticles were very stable and well-dispersed in aqueous solution, and represented minimal cytotoxicity of endothelial cells. They also demonstrated that this engineered system is able to deliver VEGF gene into endothelial cells with high efficiency. VEGF could be expressed in a sustained model after transfection. Furthermore, the multifunctional nanoparticles are extremely versatile and have great potential as probes in MR imaging and fluorescence imaging as well as gene delivery carriers due to their superparamagnetic, fluorescent and PAH positive charge. The present nanoparticle complex system is a good candidate as a theranostic agent, and has high potential in future medical applications.

Acknowledgement

The authors would like to thank S Bao and F Gao for their assistance in SEM and MR imaging experiments, respectively.

Declaration of interest

Financial support was provided, in whole or in part, by the National Natural Science Foundation of China (81071257, 81101147), the New Century Excellent Talents Program in Chinese Universities (NCET-09-0263), the Sichuan Youth Science and Technology Foundation of China (2010JQ0004), Postdoctoral Program of China (2011M501297) and The Fundamental Research Funds for Central Universities (ZYGX2010X019, ZYGX2010J101, ZYGX2011J099), are greatly appreciated.

Bibliography

1. Koransky ML, Robbins RC, Blau HM. VEGF gene delivery for treatment of ischemic cardiovascular disease. Trends Cardiovasc Med 2002;12:108–14
2. Yockman JW, Kastenmeier A, Erickson HM, et al. Novel polymer carriers and gene constructs for treatment of myocardial ischemia and infarction. J Control Release 2008;132:260–6
3. Chung YC, Hsieh WY, Young TH. Polycation/DNA complexes coated with oligonucleotides for gene delivery. Biomaterials 2010;31:4194–203
4. Singh SR, Grossniklaus HE, Kang SJ, et al. Intravenous transferrin, RGD peptide and dual-targeted nanoparticles enhance anti-VEGF intraceptor gene delivery to laser-induced CNV. Gene Ther 2009;16:645–59
5. Salem AK, Searson PC, Leong KW. Multifunctional nanorods for gene delivery. Nat Mater 2003;2:668–71
6. Pan B, Cui D, Sheng Y, et al. Dendrimer-modified magnetic nanoparticles enhance efficiency of gene delivery system. Cancer Res 2007;67:8156–63
7. Pack DW, Hoffman AS, Pun S, et al. Design and development of polymers for gene delivery. Nat Rev Drug Discov 2005;4:581–93
8. Al-Deen FN, Ho J, Selomulya C, et al. Superparamagnetic nanoparticles for effective delivery of malaria DNA vaccine. Langmuir 2011;27:3703–12
9. Chorny M, Polyak B, Alferiev IS, et al. Magnetically driven plasmid DNA delivery with biodegradable polymeric nanoparticles. FASEB J 2007;21:2510–19
10. Dave SR, Gao X. Monodisperse magnetic nanoparticles for biodetection, imaging, and drug delivery: a versatile and evolving technology. Wiley Interdiscip Rev Nanomed Nanobiotechnol 2009;1:583–609
11. Khan AA, Paul A, Abbasi S, et al. Mitotic and antiapoptotic effects of nanoparticles coencapsulating human VEGF and human angiopoietin-1 on vascular endothelial cells. Int J Nanomed 2011;6:1069–81
12. Namgung R, Singha K, Yu MK, et al. Hybrid superparamagnetic iron oxide nanoparticle-branched polyethylenimine magnetoplexes for gene transfection of vascular endothelial cells. Biomaterials 2010;31:4204–13
13. Plank C, Schillinger U, Scherer F, et al. The magnetofection method: using magnetic force to enhance gene delivery. Biol Chem 2003;384:737–47
14. Lu CW, Hung Y, Hsiao JK, et al. Bifunctional magnetic silica nanoparticles for highly efficient human stem cell labeling. Nano Lett 2007;7:149–54
15. Yu SY, Zhang HJ, Yu JB, et al. Bifunctional magnetic-optical nanocomposites: grafting lanthanide complex onto core-shell magnetic silica nanoarchitecture. Langmuir 2007;23:7836–40
16. Xiao Q, Xiao C. Preparation and characterization of silica-coated magnetic-fluorescent bifunctional microspheres. Nanoscale Res Lett 2009;4:1078–84
17. Lee JE, Lee N, Kim H, et al. Uniform mesoporous dye-doped silica nanoparticles decorated with multiple magnetite nanocrystals for simultaneous enhanced magnetic resonance imaging, fluorescence imaging, and drug delivery. J Am Chem Soc 2010;132:552–7
18. Kim J, Piao Y, Hyeon T. Multifunctional nanostructured materials for multimodal imaging, and simultaneous imaging and therapy. Chem Soc Rev 2009;38:372–90
19. Lee DE, Koo H, Sun IC, et al. Multifunctional nanoparticles for multimodal imaging and theragnosis. Chem Soc Rev 2012;41:2656–72
20. Sajja HK, East MP, Mao H, et al. Development of multifunctional nanoparticles for targeted drug delivery and noninvasive imaging of therapeutic effect. Curr Drug Discov Technol 2009;6:43–51
21. Kateb B, Chiu K, Black KL, et al. Nanoplatforms for constructing new approaches to cancer treatment, imaging, and drug delivery: what should be the policy? Neuroimage 2011;54(Suppl 1):S106–24
22. Sumer B, Gao J. Theranostic nanomedicine for cancer. Nanomedicine (Lond) 2008;3:137–40
23. Zhang G, Feng J, Lu L, et al. Fluorescent magnetic nanoprobes: design and application for cell imaging. J Colloid Interface Sci 2010;351:128–33
24. Yang J, Lee J, Kang J, et al. Magnetic sensitivity enhanced novel fluorescent magnetic silica nanoparticles for biomedical applications. Nanotechnology 2008;19:075610
25. Shi M, Liu Y, Xu M, et al. Core/shell Fe3O4 @SiO2 nanoparticles modified with PAH as a vector for EGFP plasmid DNA delivery into HeLa cells. Macromol Biosci 2011;11:1563–9
26. Lin YS, Wu SH, Hung Y, et al. Multifunctional composite nanoparticles: magnetic, luminescent, and mesoporous. Chem Mater 2006;18:5170–2
27. Wan J, Meng X, Liu E, et al. Incorporation of magnetite nanoparticle clusters in fluorescent silica nanoparticles for high-performance brain tumor delineation. Nanotechnology 2010;21:235104
28. Ou M, Kim TI, Yockman JW, et al. Polymer transfected primary myoblasts mediated efficient gene expression and angiogenic proliferation. J Control Release 2010;142:61–9
29. Zhang M, Cushing BL, O'Connor CJ. Synthesis and characterization of monodisperse ultra-thin silica-coated magnetic nanoparticles. Nanotechnology 2008;19:085601
30. Liu G, Wu H, Zheng H, et al. Synthesis and applications of fluorescent-magnetic-bifunctional dansylated Fe_3O_4@SiO_2 nanoparticles. J Mater Sci 2011;46:5959–68
31. Salgueirino-Maceira V, Correa-Duarte MA, Spasova M, et al. Composite silica spheres with magnetic and luminescent functionalities. Adv Funct Mater 2006;16:509–14
32. Wang Y, Ng YW, Chen Y, et al. Formulation of superparamagnetic iron oxides by nanoparticles of biodegradable polymers for magnetic resonance imaging. Adv Funct Mater 2008;18:308–18
33. Yoon TJ, Yu KN, Kim E, et al. Specific targeting, cell sorting, and bioimaging with smart magnetic silica core-shell nanomaterials. Small 2006;2:209–15

34. Gratton SE, Ropp PA, Pohlhaus PD, et al. The effect of particle design on cellular internalization pathways. Proc Natl Acad Sci USA 2008;105:11613–18

35. Zhang X, Meng L, Wang X, et al. Preparation and cellular uptake of pH-dependent fluorescent single-wall carbon nanotubes. Chemistry (Easton) 2010;16:556–61

36. Yang H, Lou C, Xu M, et al. Investigation of folate-conjugated fluorescent silica nanoparticles for targeting delivery to folate receptor-positive tumors and their internalization mechanism. Int J Nanomedicine 2011;6:2023–32

Affiliation

Yiyao Liu[†1] PhD, Mengran Shi[2], Mingming Xu[2], Hong Yang[2] & Chunhui Wu[2]
[†]Author for correspondence
[1]Professor,
University of Electronic Science and Technology of China,
School of Life Science and Technology,
Department of Biophysics,
Chengdu 610054,
Sichuan, P.R. China
Tel: +86 28 8320 3353;
Fax: +86 28 8320 8238;
E-mail: liuyiyao@hotmail.com
[2]University of Electronic Science and Technology of China,
School of Life Science and Technology,
Department of Biophysics,
Chengdu 610054,
Sichuan, P.R. China